

Hot drought reduces the effects of elevated CO₂ on tree water-use efficiency and carbon metabolism

Benjamin Birami¹ , Thomas Nägele^{2,3} , Marielle Gattmann¹ , Yakir Preisler⁴ , Andreas Gast¹,
Almut Arneht¹  and Nadine K. Ruehr¹ 

¹Institute of Meteorology and Climate Research – Atmospheric Environmental Research, Karlsruhe Institute of Technology KIT, Garmisch-Partenkirchen 82467, Germany; ²Department of Biology I, Plant Evolutionary Cell Biology, Ludwig-Maximilian University Munich, Planegg 82152, Germany; ³Department of Ecogenomics and Systems Biology, University of Vienna, Vienna 1090, Austria; ⁴Department of Environmental Sciences and Energy Research, Weizmann Institute of Science, Rehovot 76100, Israel

Summary

Author for correspondence:
Benjamin Birami
Tel: +49 8821 183 215
Email: benjamin.birami@kit.edu

Received: 26 September 2019
Accepted: 28 January 2020

New Phytologist (2020) 226: 1607–1621
doi: 10.1111/nph.16471

Key words: carbon balance, drought, elevated CO₂, heat, photosynthesis, primary metabolites, protein, respiration.

- Trees are increasingly exposed to hot droughts due to CO₂-induced climate change. However, the direct role of [CO₂] in altering tree physiological responses to drought and heat stress remains ambiguous.
- *Pinus halepensis* (Aleppo pine) trees were grown from seed under ambient (421 ppm) or elevated (867 ppm) [CO₂]. The 1.5-yr-old trees, either well watered or drought treated for 1 month, were transferred to separate gas-exchange chambers and the temperature gradually increased from 25°C to 40°C over a 10 d period. Continuous whole-tree shoot and root gas-exchange measurements were supplemented by primary metabolite analysis.
- Elevated [CO₂] reduced tree water loss, reflected in lower stomatal conductance, resulting in a higher water-use efficiency throughout amplifying heat stress. Net carbon uptake declined strongly, driven by increases in respiration peaking earlier in the well-watered (31–32°C) than drought (33–34°C) treatments unaffected by growth [CO₂]. Further, drought altered the primary metabolome, whereas the metabolic response to [CO₂] was subtle and mainly reflected in enhanced root protein stability.
- The impact of elevated [CO₂] on tree stress responses was modest and largely vanished with progressing heat and drought. We therefore conclude that increases in atmospheric [CO₂] cannot counterbalance the impacts of hot drought extremes in Aleppo pine.

Introduction

Forests are exposed to a rapidly changing climate world-wide, and extreme weather events such as heatwaves and drought spells are predicted to increase in frequency and severity as atmospheric [CO₂] a[CO₂] is rising (Coumou & Rahmstorf, 2012; Baldwin *et al.*, 2019; Pfliegerer *et al.*, 2019). This has pronounced impacts on forest carbon (C) and water (H₂O) cycling (Williams *et al.*, 2013), particularly in already H₂O-limited ecosystems (Choat *et al.*, 2018). Yet, the interacting effects of elevated [CO₂] (e[CO₂]) with extreme environmental conditions (such as drought, heat stress, and the combination of both) on tree stress resistance are far from clear.

Heatwaves during extended drought periods can be a main cause of forest decline (Anderegg *et al.*, 2013). Hot droughts are particularly stressful because evaporative demand is high, while H₂O availability is low and trees need to tightly regulate H₂O loss (Ameye *et al.*, 2012; Ruehr *et al.*, 2016; Birami *et al.*, 2018). This typically induces stomatal closure to maintain the integrity of the H₂O transporting system (Tyree & Zimmermann, 2002). Simultaneously, C assimilation rates decline while C is needed to

support osmoregulation and cellular maintenance (Hsiao, 1973; Huang *et al.*, 2012; Hartmann & Trumbore, 2016). Therefore, a C imbalance can arise under progressing stress, which triggers a cascade of metabolic adjustments.

A driving force of metabolic activity in plants is respiration. Typically, *c.* 30–80% of the daily photosynthetic C gain is released back to the atmosphere (Atkin & Tjoelker, 2003). During stressful conditions, the amount of respiration to assimilation can change dramatically and trees can become a net source of CO₂. It has been shown that the C loss in trees subjected to higher temperatures and increasing drought is larger and occurs earlier than under cooler conditions. This was due to respiration continuing at relatively high rates whereas assimilation started to decline earlier in drought-treated trees grown under 35°C compared with 25°C (Zhao *et al.*, 2013). Other work has shown that respiration can strongly increase under rapid warming, even in combination with drought, until rates drop at very high temperatures (Gauthier *et al.*, 2014). By contrast, if trees are exposed to elevated growth temperatures, respiration typically acclimates, nearly offsetting the effect of the warming (Reich *et al.*, 2016; Drake *et al.*, 2019). Although much research has focused on the

temperature relationship of respiration, we have little mechanistic understanding to predict how respiration will respond to day-long heatwaves, let alone in combination with drought and/or changes in $[\text{CO}_2]$.

Increasing $a[\text{CO}_2]$ may affect tree stress responses through a variety of plant physiological processes. For instance, $e[\text{CO}_2]$ often suppresses photorespiration and dark respiration (Drake *et al.*, 1999; Dusenge *et al.*, 2019), whereas it stimulates C assimilation and productivity under nonstressful conditions (Ainsworth & Long, 2005; Ainsworth & Rogers, 2007; Ameye *et al.*, 2012; Simón *et al.*, 2018; Zinta *et al.*, 2018). Alongside increases in C uptake, stomatal conductance g_s typically declines (Eamus, 1991). This reduction in g_s corresponds with a larger leaf-intercellular $[\text{CO}_2]$ C_i , stimulated photosynthesis, and increased plant H_2O -use efficiency (WUE) – the ratio of C uptake via assimilation per unit H_2O loss from transpiration (Lavergne *et al.*, 2019). Increases in WUE under $e[\text{CO}_2]$ have been observed in many studies (Eamus, 1991), particularly in H_2O -limiting environments (Wullschlegel *et al.*, 2002). However, the combined effects of $e[\text{CO}_2]$ stress responses during extreme heat and/or drought stress have rarely been investigated, and results remain inconclusive. For instance, $e[\text{CO}_2]$ could not mitigate extreme drought stress (withholding H_2O until mortality occurred) in *Pinus radiata* and *Callitris rhomboidea* (Duan *et al.*, 2015) or in *Eucalyptus globulus* when +240 ppm CO_2 was combined with a constant +4°C warming (Duan *et al.*, 2014), whereas it alleviated extreme heat stress in *Pinus taeda* and *Quercus rubra* (Ameye *et al.*, 2012; +320 ppm, +12°C heatwave) and *Larrea tridentata* (Hamerlynck *et al.*, 2000; +340 ppm CO_2 , +8°C heatwave).

A more comprehensive picture on the interacting effects of $e[\text{CO}_2]$ on plant stress performance could be gained through a whole-tree C perspective – integrating sink and source responses (Dusenge *et al.*, 2019; Ryan & Asao, 2019). Moreover, investigating changes in the primary metabolism could allow identification of some of the underlying mechanisms (Xu *et al.*, 2015; Mohanta *et al.*, 2017). For instance, $e[\text{CO}_2]$ can increase sugar and starch concentrations, which might buffer plant C losses during drought via enhanced C supply and/or improved osmoregulation (Ainsworth & Long, 2005; Ainsworth & Rogers, 2007) as well as may reduce oxidative stress (Zinta *et al.*, 2014). However, $e[\text{CO}_2]$ may also affect the C : nitrogen (N) stoichiometry and N dilution, as has been observed, resulting in decreased protein and amino acid concentrations (Poorter *et al.*, 1997; Johnson & Pregitzer, 2007). A decrease in protein content may affect assimilation and respiration rates (Drake *et al.*, 1999; Xu *et al.*, 2015; Dusenge *et al.*, 2019), could dampen stress-induced upregulation of amino acids important for osmoregulation (Zinta *et al.*, 2018), and may affect the abundance of heat-shock proteins, and therefore plant thermotolerance (Coleman *et al.*, 1991; Huang *et al.*, 2012; Zhang *et al.*, 2018). Hence, $e[\text{CO}_2]$ can trigger metabolic processes that may directly interact with tree drought and heat stress responses. Yet, results remain inconclusive because we miss an integrated understanding of the interactive effects of $e[\text{CO}_2]$ and stress on the C balance and primary metabolism of trees.

Here, we provide novel insights into the impacts of $e[\text{CO}_2]$ on whole-tree shoot and root stress responses in Aleppo pine saplings

originating from a semi-arid forest at the arid timberline (Grünzweig *et al.*, 2009). To elucidate the effects of $[\text{CO}_2]$ in combination with drought and heat stress on physiological responses, we combined measurements of whole-tree C balance, WUE, and primary metabolites. More specifically, our hypotheses were as follows: first, that $e[\text{CO}_2]$ increases photosynthesis, which results in a larger net C uptake maintained during heat stress; second, that WUE increases proportionally with $a[\text{CO}_2]$ and that this increase can be maintained during heat stress but not during hot drought, when stomata are closed; and third, the tree metabolic response to temperature is suppressed under $e[\text{CO}_2]$, which is reflected in a concurrent change in respiratory activity and primary metabolites.

Materials and Methods

Plant material

Pinus halepensis (Miller) saplings were grown from seeds for 18 months under ambient CO_2 (*c.* 420 ppm) or $e[\text{CO}_2]$ (*c.* 870 ppm, within the range of representative concentration pathway 8.5 for 2100; IPCC, 2014) in a scientific glasshouse facility in Garmisch-Partenkirchen, Germany (732 m asl, 47°28'32.87"N, 11°3'44.03"E) with highly UV-transmissive glass (70%). The origin of the seed material is a 50-yr-old Aleppo pine plantation in Israel (Yatir Forest). Cones of trees were sampled growing in close proximity to a meteorological station and flux tower (IL-Yat, 650 m asl, 31°20'49.2"N, 35°03'07.2"E).

In the following, the experimental design of the study is explained in detail from the germination of the seedlings until the 18-month-old saplings were transferred into separate tree gas-exchange chambers (see Fig. 1). Seeds germinated on vermiculite in two transparent growth chambers either under ambient $[\text{CO}_2]$ or $e[\text{CO}_2]$. About 10 wk after germination, in July 2016, the seedlings were transferred to pots ($5 \times 5 \times 5 \text{ cm}^3$, 0.125 l) containing a C-free potting mixture of 1 : 1 : 0.5 quartz sand (0.7 mm and 1–2 mm), vermiculite (*c.* 3 mm), and quartz sand (Dorsolit 4–6 mm) with 1 cm of expanded clay (8–16 mm) as a drainage. Seedlings were fertilized with 2 g of slow-release fertilizer (Osmocote® Exact 3-4M 16-9-12 + 2MgO+TE; ICL Specialty Fertilizers, Heerlen, the Netherlands) supplemented by liquid fertilizer (Manna® Wuxal Super; Wilhelm Haug GmbH & Co. KG, Ammerbuch, Germany). Placement of the seedlings within the two growth chambers was randomized every second week; and to overcome a possible chamber effect, the CO_2 treatments were moved at monthly intervals between the chambers (Fig. 1). After the saplings were 7 months old they were placed in two glasshouse compartments referring either to $a[\text{CO}_2]$ and $e[\text{CO}_2]$ conditions and 10-month-old seedlings were individually transferred to larger pots (4.5 l) for a second time. The potting mixture was again a C-free substrate of 1 : 1 : 2 vermiculite (3–6 mm), coarse (4–6 mm), and fine quartz sand (2–3 mm) with 1 cm of expanded clay (8–16 mm) as a drainage. Slow-release fertilizer (5 g, Osmocote® Exact Standard 5-6M 15-9-12+2MgO+TE; ICL Specialty Fertilizers) was added to the mixture and supplemented by liquid fertilizer, phosphate, and

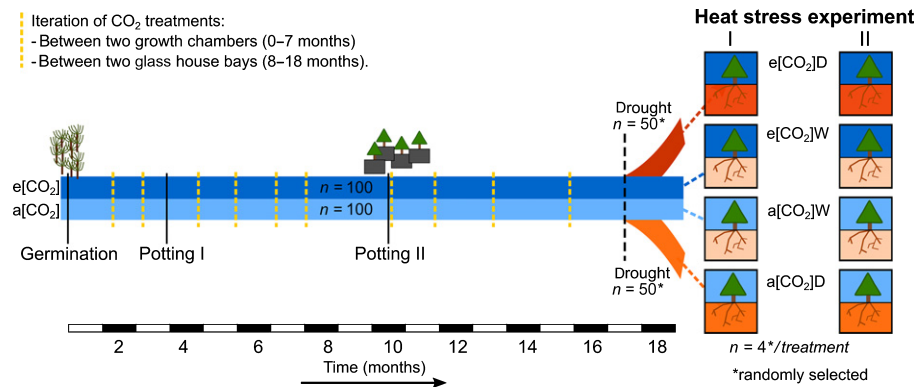


Fig. 1 Experimental timeline from seedling (*Pinus halepensis*) germination until two heat experiments (each 10 d) were conducted 18 months later. The initiation of the CO₂ (elevated [CO₂] (e[CO₂]: dark blue; atmospheric [CO₂] (a[CO₂]): light blue) and drought treatments (orange) is also shown. Seedlings of the four treatments (a[CO₂]W, e[CO₂]W, a[CO₂]D, e[CO₂]D; D, drought; W, well-watered) were randomly selected and transferred to the gas-exchange chambers where temperature was increased stepwise (25°C, 30°C, 35°C, 38°C, 40°C) and above and belowground gas-exchange measured. The heat experiment was repeated with a new set of seedlings to increase number of replicates to eight per treatment. Note that one gas-exchange chamber per treatment was left blank to serve as a quality control. The yellow dotted lines depict iteration of the CO₂ treatments between two growth chambers or two glasshouse bays.

magnesium addition once. Incoming light from outside was supplemented with plant growth-lamps (T-agro 400 W; Philips, Hamburg, Germany) and the saplings were irrigated regularly to saturation. A possible effect of the placement within the glasshouse was again overcome by iterating the CO₂ treatments between the two glasshouse bays four times before the start of the heat stress experiment in September 2017 (Fig. 1).

Atmospheric CO₂ differed greatly between the glasshouse compartments (421 ± 105 ppm in a[CO₂] and 867 ± 157 ppm in e[CO₂] on average, increase in [CO₂] of 106% during growth period), whereas all other growth conditions were kept similar (see Supporting Information Fig. S1). Moisture sensors (10HS; Decagon Devices Inc., Pullman, WA, USA; calibrated to potting substrate) and an automated drip irrigation system were installed (Rain Bird, Azusa, CA, USA) when seedlings were 15 months old. The irrigation was adapted to result in a relative substrate H₂O content (RSWC) of 50% (Fig. S2) close to the soil H₂O content in the Yatir Forest during spring conditions. RSWC was calculated as follows:

$$RSWC = 100 \times \frac{SWC_{\text{sample}} - SWC_{\text{min}}}{SWC_{\text{max}} - SWC_{\text{min}}} \quad \text{Eqn 1}$$

(SWC_{max} (g g⁻¹), maximum amount of H₂O held by the substrate (e.g. field capacity); SWC_{min} (g g⁻¹), minimum amount of H₂O held by the substrate, set to zero; SWC_{sample}, measured substrate H₂O content, derived from the calibrated moisture sensors).

When seedlings were about 17 months old, half of the seedlings from each CO₂ treatment were randomly selected and assigned to a drought treatment (D). In the drought trees, irrigation was slowly reduced to maintain daily-averaged RSWC at c. 10%, whereas RSWC in the well-watered trees (W) was maintained at 50%, leading to a pronounced decrease in H₂O potential. Two sets of seedlings from each of the four treatments (a[CO₂]W, e[CO₂]W, a[CO₂]D, e[CO₂]D) were randomly

selected 40 d and 50 d after drought had been initiated (Fig. 1), transferred to custom-built separate tree gas-exchange chambers (see section Chamber system) and exposed to increasing heat stress (n = 4 per treatment) for a period of 10 d.

Tree gas-exchange chambers

Chamber system We developed a tree gas-exchange system with 20 separate chambers divided into above and belowground compartments to continuously measure the exchange of H₂O and CO₂. Each of the 20 aboveground compartments were individually temperature-controlled (Fig. 2). The aboveground and belowground compartments were separated and gas tightness between the above- and belowground compartment was ensured after enclosing the tree stem. For details on the set-up and constant air supply of the tree gas-exchange system, see S1.

The chamber system was installed in the glasshouse and outside light was supplemented with plant growth lamps (T-agro 400 W; Philips, Hamburg, Germany). Canopy light conditions inside each chamber were measured automatically with a photodiode (G1118; Hamamatsu Photonics, Hamamatsu, Japan), which had been cross-calibrated with a high-precision photosynthetic active radiation (PAR) sensor (PQS 1; Kipp & Zonen, Delft, the Netherlands). Root-zone conditions were monitored with temperature sensors (TS 107; Campbell Scientific Inc., Logan, UT, USA) and moisture sensors (10HS; Decagon Devices Inc.). These data were logged half-hourly (CR1000; Campbell Scientific Inc.).

Gas-exchange measurements The gas-exchange chambers were constantly supplied with an air stream (Air_{supply}) of either 408 ppm or 896 ppm CO₂. Sample air (Air_{sample}) was drawn at a rate of 500 ml min⁻¹, and each seedling was measured once every 80 min using differential gas analysis. We used two gas analyzers: the analyzer measuring absolute [CO₂] and [H₂O] (LI-840; Licor, Lincoln, NE, USA) was connected to a differential gas

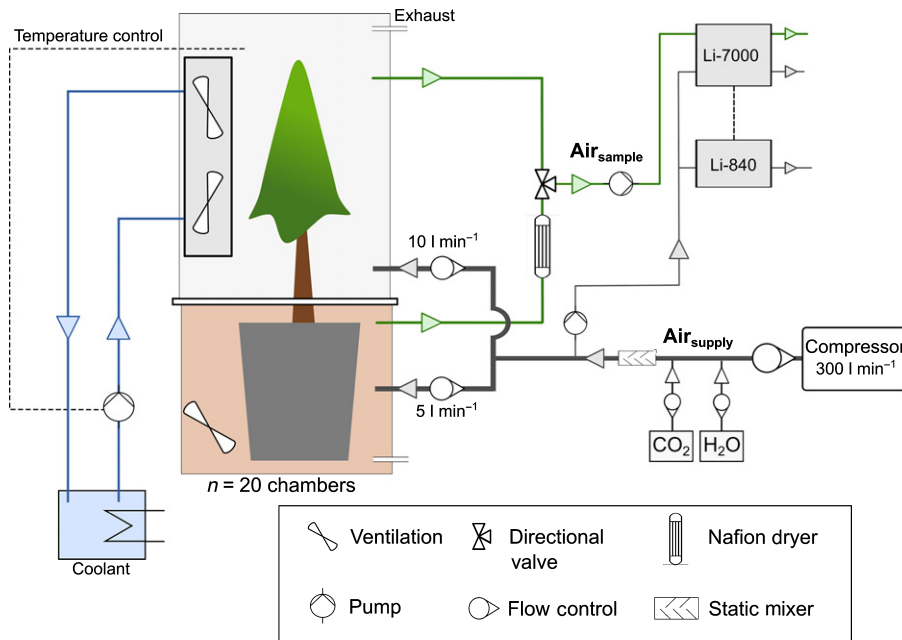


Fig. 2 Whole-tree gas-exchange system separated in an above and belowground compartment, shown exemplified for one chamber ($n = 20$ in total). The arrows indicate the direction of flow. The air supply to the chambers is given in black (Air_{supply}), and the sample air is given in green (Air_{sample}). The Li-840 measured absolute $[CO_2]$ and $[H_2O]$ connected to an Li-7000 to measure differences between Air_{supply} and Air_{sample} . Note that trees (*Pinus halepensis*) were potted in carbon-free substrate and the belowground CO_2 efflux is therefore interpreted as root respiration.

analyzer (Li-7000; Li-Cor) quantifying $[CO_2]$ and $[H_2O]$ differences between Air_{supply} and Air_{sample} . The data were logged at 10 s intervals. The gas analyzers were calibrated following the manufacturer's recommendations.

To eliminate any offset between Air_{supply} and Air_{sample} not caused by plant gas-exchange, empty aboveground and belowground compartments ($n = 1$ per treatment, four in total) containing C-free potting substrate only, were measured and offsets (on average $+0.33 \pm 1.2$ ppm CO_2 and 0.02 ± 0.05 ppt H_2O in the aboveground compartments) removed accordingly. Differences in CO_2 were slightly larger in the belowground compartments ($c. +2$ ppm on average) and may be due to some microbial activity in the potting substrate.

Gas-exchange fluxes of CO_2 and H_2O were calculated from the concentration differences between Air_{supply} and Air_{sample} . Plant H_2O loss via transpiration E ($mol\ s^{-1}$) was calculated as follows:

$$E = \frac{\dot{m}(W_{sample} - W_{supply})}{1 - W_{sample}} \quad \text{Eqn 2}$$

(\dot{m} , air mass flow ($mol\ s^{-1}$) into the chamber compartment; W_{sample} , H_2O vapor concentration of Air_{sample} ($mol\ mol^{-1}$); W_{supply} , H_2O vapor concentration of Air_{supply} ($mol\ mol^{-1}$)).

From daytime E and H_2O vapor concentrations we determined stomatal conductance g_s ($mol\ s^{-1}$) as follows:

$$g_s = \frac{E \left(1000 - \frac{W_{leaf} + W_{sample}}{2} \right)}{W_{leaf} - W_{sample}} \quad \text{Eqn 3}$$

(W_{leaf} ($mol\ mol^{-1}$), leaf H_2O vapor concentration, derived from the ratio of saturation vapor pressure (kPa) at a given air temperature ($^{\circ}C$) and atmospheric pressure). This

approach, which neglects boundary-layer conductance, is suitable under well-coupled conditions, as confirmed by negligible temperature differences between chamber and tree canopy ($< 1^{\circ}C$; see Table S1).

CO_2 gas exchange ($mol\ s^{-1}$) – that is, net photosynthesis A_{Net} , shoot respiration R_{shoot} , and root respiration R_{root} – was calculated as follows:

$$CO_2 \text{ flux} = -\dot{m}(C_{sample} - C_{supply}) - (EC_{sample}) \quad \text{Eqn 4}$$

(C_{sample} , $[CO_2]$ of Air_{sample} ($mol\ mol^{-1}$); C_{supply} , $[CO_2]$ of Air_{supply} ($mol\ mol^{-1}$); E , used to correct for dilution through transpiration ($mol\ s^{-1}$)). In the case of R_{root} (where sample air was dried), the H_2O vapor dilution term became negative. The daily net C uptake (mg) per tree was calculated based on daily-averaged A_{Net} and respiration as follows:

$$C_{Net} = A_{Net} - (R_{shoot} + R_{root}) \quad \text{Eqn 5}$$

In order to determine changes in whole-tree WUE, apparent WUE was derived as follows:

$$WUE_a = \frac{A_{net}}{E_{day}} \quad \text{Eqn 6}$$

To allow comparison of tissue gas-exchange activity between treatments and because root surface area was not available, we calculated gas-exchange rates per shoot (i.e. needle and woody tissues) or root DW, if not stated otherwise. The percentage share of soluble C from tissue biomass was small ($< 4\%$; Table S2), hence we refrained from taking normalization to soluble C into account. Tree biomass was determined at the end of the experiment and separated into needles, roots, and woody tissues before drying at $60^{\circ}C$ for 48 h (Table 1).

Heat stress experiment

Responses of shoot and root gas-exchange with increasing temperature and evaporative demand were assessed continuously using the tree gas-exchange system described in the Tree gas-exchange chambers section and Notes S1. In brief, randomly selected seedlings were placed into separate gas-exchange chambers ($n = 4$ per treatment, Fig. 1). The chambers containing one tree each were positioned next to each other in a randomized block design. The heat stress experiment was repeated in order to double the numbers of replicates per treatment. Each heat experiment lasted 10 d, and after the initial 2 d at 25°C (20°C nighttime) the temperature was increased stepwise every second day to the following daytime temperatures: 25, 35, 38, and 40°C (Fig. 3a). We refrained from temperatures above 40°C as tree mortality has been found to strongly increase in Aleppo pine seedlings above this threshold, particularly in combination with drought (Birami *et al.*, 2018). As during a typical heatwave in the Yatir Forest (Tatarinov *et al.*, 2016), vapor pressure deficit (VPD) increased alongside increasing temperature, and this increase was slightly greater in the drought-treated saplings due to low E (Fig. 3c). PAR was kept relatively constant between gas-exchange chambers, and daily averages were $456 \pm 140 \mu\text{mol m}^{-2} \text{s}^{-1}$. To overcome some of the light limitations (saturating PAR for photosynthesis was at $1200 \mu\text{mol m}^{-2} \text{s}^{-1}$) daytime length was set to 16 h, well above the average summer day length in Yatir Forest. Irrigation was controlled to maintain the RSWC of well-watered trees at *c.* 50% and of drought-treated trees at *c.* 10% (Fig. 3). The irrigation amount did not differ between the $[\text{CO}_2]$ treatments (a $[\text{CO}_2]$ W and e $[\text{CO}_2]$ W: 300 ml d^{-1} ; a $[\text{CO}_2]$ D and e $[\text{CO}_2]$ D: 50 ml d^{-1}) and drought-treated seedlings reached a midday needle H_2O potential ψ_{midday} indicating stomatal closure (Fig. S3; Table 2).

Sample preparation

We sampled needle tissue for analysis of primary metabolites on the last day of the following temperature levels: 25, 35, 38 and 40°C. To avoid disturbance of belowground fluxes, root biomass was only sampled at 25°C (additional set of saplings, not used for the experiments) and at 40°C. Sampling took place in the

afternoon between 15:00 h and 16:00 h; samples were immediately frozen in liquid N_2 and then stored at -80°C until ground to fine powder in liquid N_2 before freeze-drying for 72 h with cooling aggregate at -80°C and sample temperature at -30°C (Alpha 24 LSC; Martin Christ Gefriertrocknungsanlagen GmbH, Osterode am Harz, Germany). The freeze-dried samples were stored in the dark in closed vials at room temperature, and analyses of primary metabolites were completed within 2 months (Fürtauer *et al.*, 2019). For details on analysis of primary metabolites via gas chromatography coupled with time-of-flight mass spectrometry (Fürtauer *et al.*, 2016; Weiszmann *et al.*, 2018) and protein content via Bradford assay (Fürtauer *et al.*, 2018), please see Notes S2.

Statistical data analysis

Data processing, analysis, and statistics were carried out using R v.3.5.2 (R Core Team, 2018). Gas-exchange measurements of each chamber were carefully inspected before analyses, and day or nighttime fluxes outside 1.5 times the interquartile range (above the upper quartile and below the lower quartile) per temperature were considered outliers. This removed, on average, 3.8% of CO_2 and 5.7% of H_2O gas-exchange data.

Primary metabolites were scaled to SD before treatment effects in needles and roots at 25°C were visualized by hierarchical clustering, utilizing R packages GGPlot2 (Wickham, 2016) and CLUSTER (Maechler *et al.*, 2018). Further, the overall changes in the primary metabolome depending on tissue, treatment, and temperature were analyzed after centering of the scaled data via principal components analysis.

Treatment effects on biomass, gas-exchange rates, and metabolites at specific temperature levels were tested using ANOVA, and differences between treatments were revealed by post hoc analysis (Tukey honestly significant difference (HSD)). Treatment and temperature dependencies of gas-exchange fluxes and metabolites (fixed effects) were checked by implementing a linear mixed effects model (LMERTEST; Kuznetsova *et al.*, 2017). In order to account for temporal autocorrelation, tree was accounted as a random factor. Using the reduced sample size Akaike information criteria (Akaike, 1974; Giraud, 2015), the most parsimonious model was selected with or without tree as random factor,

Table 1 Needle, shoot, root, total tree biomass, needle area, and total soluble carbon (C, calculated as C equivalents of all measured metabolites) for 1.5-year-old *Pinus halepensis* seedlings are given as treatment averages ± 1 SE ($n = 16$ per treatment) at the end of the experiment (post-stress).

Treatment	Biomass (g DW)				Needle area (cm ²)	Soluble C ($\mu\text{mol g}^{-1}$ DW)
	Needle	Root	Wood	Total		
a $[\text{CO}_2]$ W	33.4 \pm 1.0 A	51.1 \pm 1.4 B	15.4 \pm 0.6 A	99.9 \pm 2.1 A	1296 \pm 38 A	1090 \pm 209 A
e $[\text{CO}_2]$ W	47.6 \pm 1.5 B	66.7 \pm 1.9 D	24.5 \pm 1.2 B	138.8 \pm 2.1 B	1925.3 \pm 84 B	847 \pm 79 A
a $[\text{CO}_2]$ D	33.3 \pm 1.5 A	43.6 \pm 1.2 A	15.8 \pm 0.9 A	92.7 \pm 2.9 A	1414.6 \pm 60 A	2623 \pm 454 B
e $[\text{CO}_2]$ D	47.5 \pm 1.4 B	60.0 \pm 2.2 C	24.2 \pm 1.4 B	131.6 \pm 4.5 B	2052.5 \pm 65 B	2578 \pm 349 B

D, drought; W, water treated; a, atmospheric; e, elevated.

Significant differences between treatments were derived from ANOVA followed by Tukey's honestly significant difference and are given in upper-case letters ($P < 0.05$).

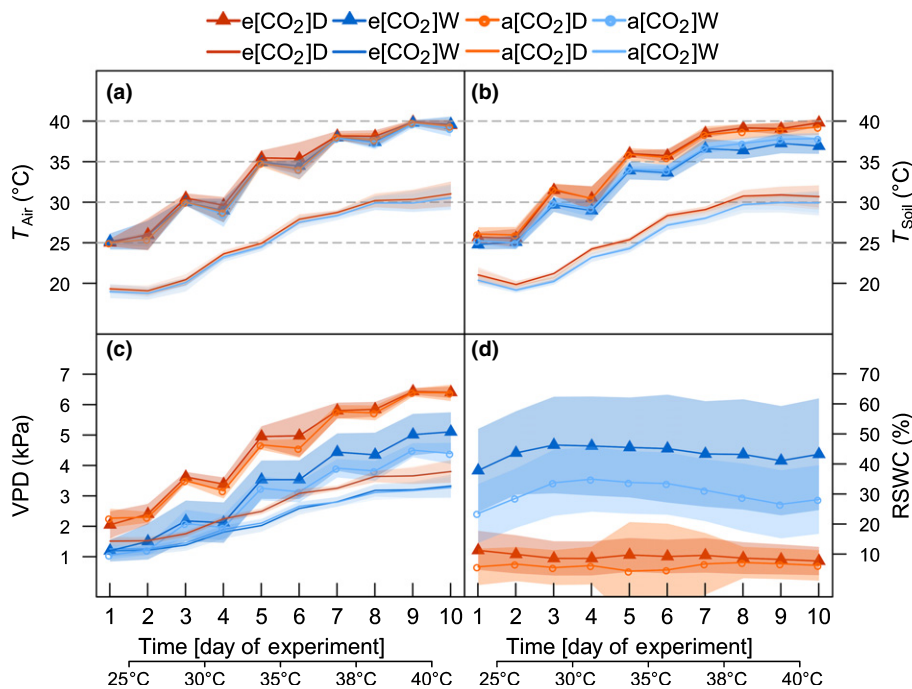


Fig. 3 Environmental drivers during the heat stress experiment (*Pinus halepensis*) given per treatment. (a) Air temperature T_{Air} , (b) soil temperature T_{Soil} , (c) vapor pressure deficit (VPD), and (d) relative substrate water content (RSWC) are shown. Data are treatment-averages during daytime (lines including symbols) or nighttime (lines), and the shaded areas are ± 1 SD ($n = 8$). Daytime is defined as photosynthetic active radiation (PAR) > 100 and nighttime as PAR = 0. Note the temperature difference between day and nighttime was not constant due to technical limitations but was kept within 7–10°C.

Table 2 Gas-exchange rates at 25°C expressed per tissue DW and tree net carbon (C) uptake for 1.5-yr-old *Pinus halepensis* seedlings given as treatment averages ± 1 SE ($n = 8$ per treatment).

Treatment	E ($\mu\text{mol s}^{-1} \text{g}^{-1}$)	g_s ($\text{mmol s}^{-1} \text{g}^{-1}$)	A_{Net} ($\text{nmol s}^{-1} \text{g}^{-1}$)	R_{dark} ($\text{nmol s}^{-1} \text{g}^{-1}$)	C_i ($\mu\text{mol mol}^{-1}$)	WUE ($\mu\text{mol mmol}^{-1}$)	Net C uptake/tree (mg d^{-1})	ψ_{midday} (MPa)
a[CO ₂]W	3.29 \pm 0.15 B	0.38 \pm 0.04 B	15.3 \pm 1.3 B	7.4 \pm 0.3 B	263 \pm 3 A	4 \pm 0.3 A	165.1 \pm 29.8 AC	-1.49 \pm 0.07 A
e[CO ₂]W	2.03 \pm 0.28 D	0.23 \pm 0.07 B	16.5 \pm 2.2 B	6 \pm 0.2 C	612 \pm 5 C	7.2 \pm 0.5 B	379.2 \pm 68.8 C	-1.15 \pm 0.04 A
a[CO ₂]D	0.66 \pm 0.17 A	0.08 \pm 0.01 A	3.4 \pm 1.1 A	3.9 \pm 0.4 A	287 \pm 11 A	3.4 \pm 0.7 A	-73.2 \pm 18.3 B	-2.68 \pm 0.3 B
e[CO ₂]D	0.67 \pm 0.16 A	0.04 \pm 0.02 A	6.7 \pm 1.2 C	4.2 \pm 0.3 A	482 \pm 14 B	9.4 \pm 1.3 B	23.2 \pm 38.7 AB	-1.83 \pm 0.2 A

D, drought; W, water treated; a, atmospheric; e, elevated.

E , transpiration; g_s , stomatal conductance; A_{Net} , net photosynthesis; R_{dark} , dark respiration; C_i , leaf-intercellular [CO₂]; WUE, water-use efficiency; ψ_{midday} , midday needle water potential.

Tree net C uptake is the sum of photosynthesis A_{Net} minus respiration R . ψ_{midday} is given and was measured at the time of tissue sampling for metabolite analysis. Significant differences between treatments were derived from ANOVA followed by Tukey's honestly significant difference and are given in upper-case letters ($P < 0.05$).

and the treatment and temperature effects included with and without interaction. We report a pseudo- R^2 (pR^2) for the selected model (MUMIN; Barton, 2019). Homoscedasticity and normality of residuals were checked and, if applicable, \log_e transformation applied.

To analyze differences in the temperature relationship of A_{Net} we applied an exponential decay function ($y = e^{-bx}$); in the case of respiration R , we fitted a second-order polynomial function following (Gauthier *et al.*, 2014):

$$R = e^{a+bT+cT^2}$$

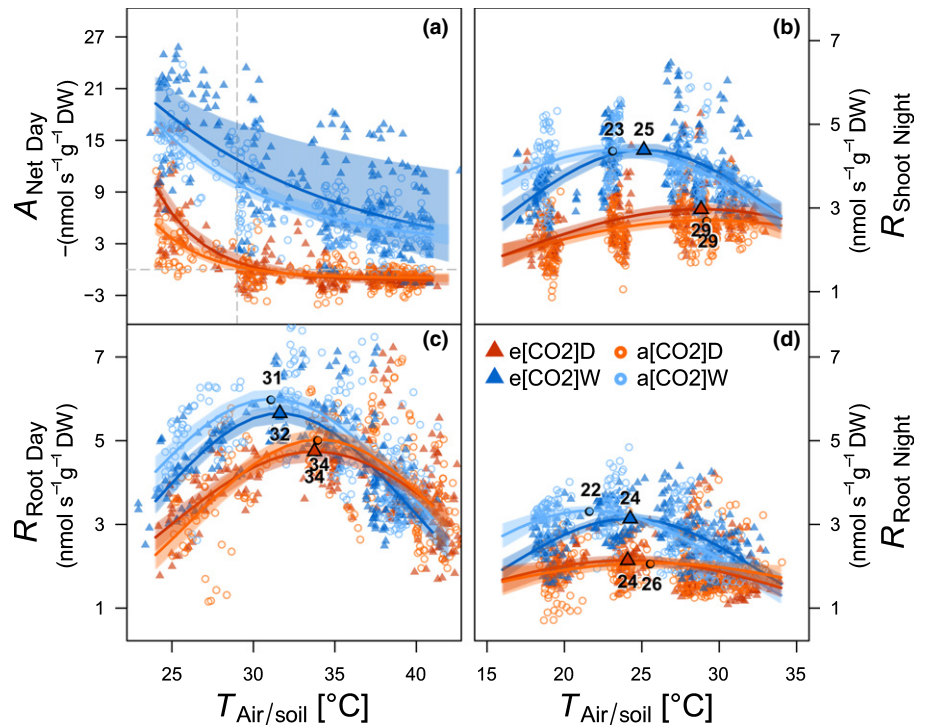
The uncertainties of all fitted functions are given as 95% confidence intervals derived from first-order Taylor expansion using the PROPAGATE package (Spiess, 2018).

Results

Tree biomass

Differences in above and belowground biomass were distinct after growing *P. halepensis* seedlings for more than 1 yr under a [CO₂] of 421 ppm or e[CO₂] of 867 ppm (Table 1). A doubling of atmospheric [CO₂] increased total tree biomass by 35%. This increase was particularly pronounced in woody tissues (stem and twigs, +47%) and to a lesser extent in needles (+26%). The 1-month drought period had no obvious effect on aboveground biomass, but reduced belowground biomass under ambient (-15%) and e[CO₂] (-11%). The amount of nonstructural carbohydrates in total biomass varied between 1.5 and 3.5% and

Fig. 4 Gas-exchange dynamics with increasing heat stress under ambient or elevated $[\text{CO}_2]$ in drought or well-watered *Pinus halepensis* trees. Shown are hourly averages per tree and treatment of (a) net photosynthesis A_{Net} , (b) shoot dark respiration R_{Shoot} , and (c) daytime (10:00 h to 18:00 h) and (d) nighttime (23:00 h to 04:00 h) root respiration R_{Root} . The temperature response of A_{Net} was fitted with an exponential decay function and respiration data fitted to a second-order polynomial function (see Eqn 6). The temperature at the respiratory peak is highlighted. The shaded areas depict the 95% confidence intervals of the fitted functions. Note that gas-exchange data are expressed per DW shoot or root tissue.



was slightly larger under drought with no clear trend of $[\text{CO}_2]$ (Table S2).

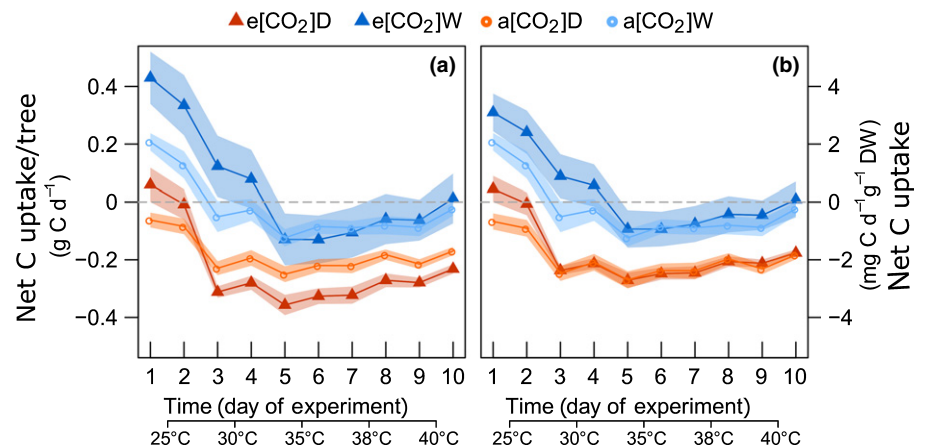
Tree gas-exchange

Impacts of $[\text{CO}_2]$ and drought Elevated $[\text{CO}_2]$ affected gas-exchange rates expressed per tissue DW (Table 2; see also Fig. 4). Under well-watered conditions and at ambient temperature (25°C), R was lower in $e[\text{CO}_2]\text{W}$ trees than in $a[\text{CO}_2]\text{W}$ trees. In addition, $e[\text{CO}_2]$ reduced g_s and E , which resulted in an increase of WUE (Table 2), whereas A_{Net} was largely unaffected (Table 2). Under drought, the effect of $[\text{CO}_2]$ on WUE was pronounced, with C_i being increased near stomatal closure, allowing for a higher A_{Net} (Table 2). The positive effect of $e[\text{CO}_2]$ on biomass, C_i , and WUE was also reflected in daily net C uptake (i.e. tree C balance), but the degree did depend on H_2O supply.

Whereas in the well-watered trees the net C uptake tended to double under $e[\text{CO}_2]$, drought trees were able to maintain a small C sink if grown under $e[\text{CO}_2]$ (Table 2).

Heat stress responses altered by $[\text{CO}_2]$ and drought Increasing temperatures affected VPD accordingly (Fig. 3c), and we found pronounced responses in gas exchange of the well-watered seedlings. A_{Net} declined with temperature irrespective of the $[\text{CO}_2]$ (Fig. 4a). This was contrasted by initially increasing C loss via R_{Root} and R_{Shoot} until a respiratory peak has been reached and respiration rates began to decline (Fig. 4b,c). This respiratory peak was reached $2\text{--}4^\circ\text{C}$ later and at lower rates in the drought-treated saplings. The trees' net C uptake reacted accordingly with a sharp initial decrease, which then leveled off at increasing heat stress ($30\text{--}35^\circ\text{C}$; Fig. 5). The effects of $e[\text{CO}_2]$ were not distinct, but data showed a tendency of whole-tree net C losses to be

Fig. 5 Temperature responses of the whole-tree carbon (C) balance (i.e. net C uptake) in *Pinus halepensis* seedlings (a) per tree and (b) DW biomass. Shown are daily averages per treatment ($a[\text{CO}_2]\text{W}$, $e[\text{CO}_2]\text{W}$, $a[\text{CO}_2]\text{D}$, $e[\text{CO}_2]\text{D}$; $a[\text{CO}_2]$, atmospheric $[\text{CO}_2]$; $e[\text{CO}_2]$, elevated $[\text{CO}_2]$; D, drought; W, well-watered). Whole-tree net C uptake was derived from hourly photosynthesis and respiration data per seedling (Eqn 5). Note that positive numbers reflect a daily net C gain, and negative numbers are a net C loss. The shaded areas are ± 1 SE ($n = 8$).



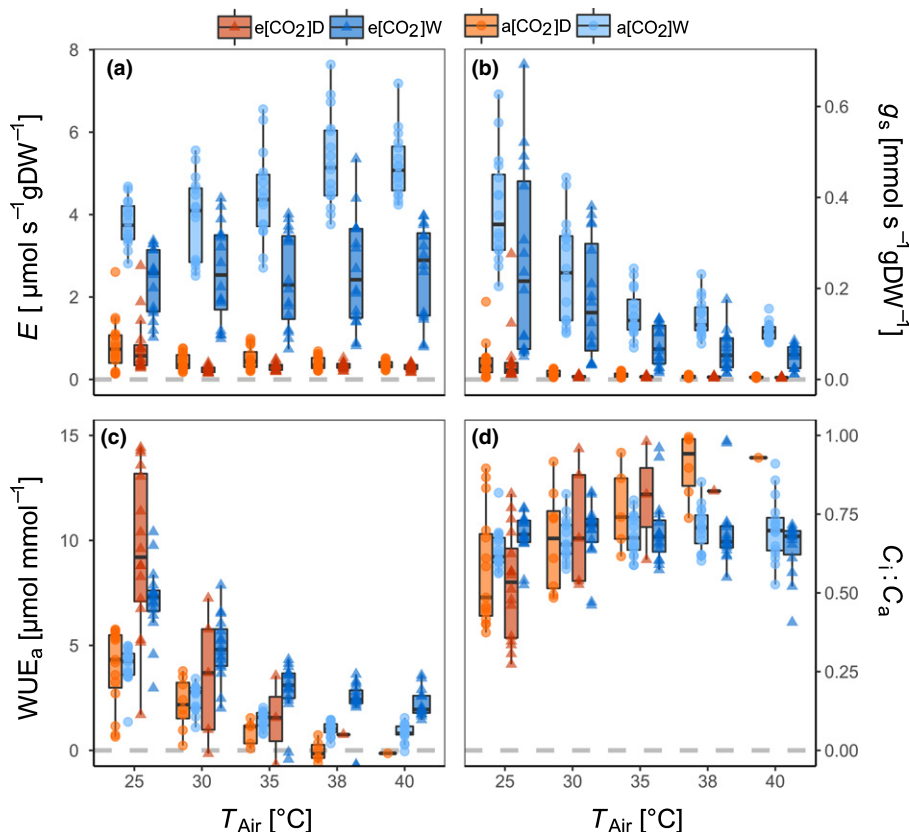


Fig. 6 Treatment responses of (a) transpiration E , (b) stomatal conductance g_s , (c) apparent water use efficiency (WUE_a), and (d) the ratio of intercellular to ambient $[CO_2]$ ($C_i : C_a$) of *Pinus halepensis* seedlings with increasing temperature. Data points are daily-averaged values per temperature level and tree (between 10:00 h and 16:00 h). WUE_a and $C_i : C_a$ are given for $C_i \leq C_a$. The relationships of hourly WUE and g_s with temperature are given in Supporting Information Fig. S4.

observed at slightly higher temperatures under both well-watered and drought conditions.

A pronounced interaction of $e[CO_2]$ with heat stress became clear in a constantly lower E (lme: $pR^2 = 0.89$; Tukey HSD, $P < 0.05$) but higher WUE (lme: $pR^2 = 0.81$; Tukey HSD, $P < 0.05$) with increasing temperatures under well-watered conditions. This was due to a tight stomatal control in the $e[CO_2]$ W trees (Fig. 6a,b; Table S3). The picture changed dramatically when heat stress was combined with drought; the H_2O -saving effect of $e[CO_2]$ quickly subsided at temperatures $> 30^\circ C$, coinciding with stomatal closure. Interestingly, the C_i to ambient $[CO_2]$ (C_a) ratio seemed largely unaffected by the $[CO_2]$ and remained almost constant throughout the experiment (Fig. 6d, excluding $C_i > C_a$).

Primary metabolites

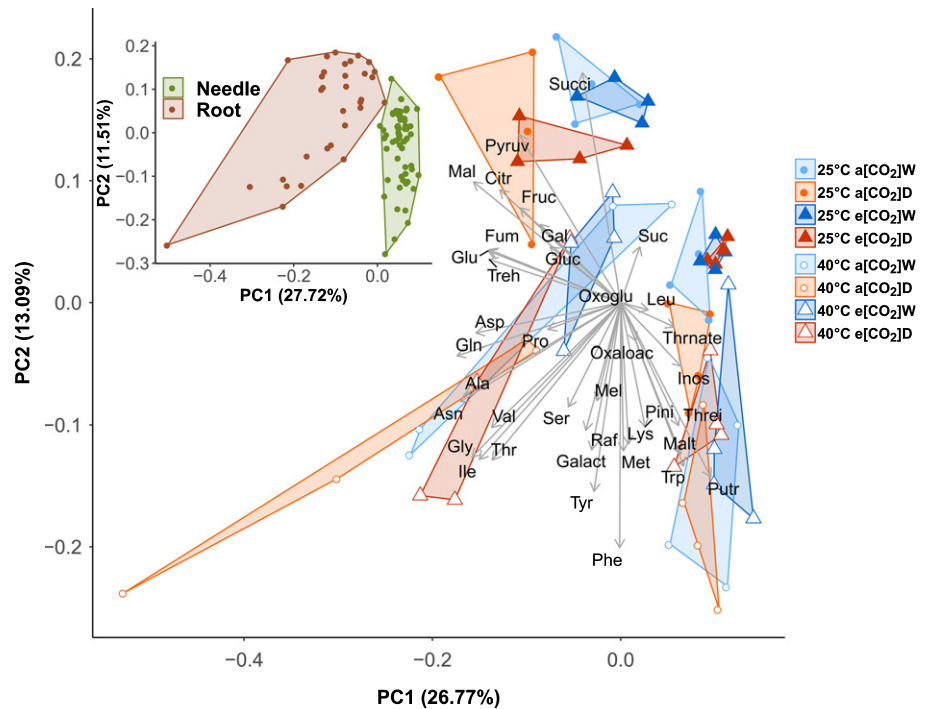
Impacts of $[CO_2]$ and drought The primary metabolism in roots and needles was clearly distinct, irrespective of treatment (Fig. 7; metabolite profile at $25^\circ C$). We found inositol pathway intermediates (e.g. *myo*-inositol, pinitol), polyamines, and aromatic amino acids to dominate in needle tissues, whereas monosaccharides, TCA intermediates (e.g. malate), and amino acids of the glutamate and aspartate family were higher concentrated in roots.

In addition, we found the metabolic responses to drought larger than the $[CO_2]$ effect, as reflected in the clustering (Fig. S5). For instance, monosaccharides (lme: $pR^2 = 0.74$) and

sucrose (lme: $pR^2 = 0.43$) were clearly enhanced under drought, accompanied by increased levels of proline in both needles (lme: $pR^2 = 0.47$; Tukey HSD, $P < 0.05$) and roots (lme: $pR^2 = 0.69$; Tukey HSD, $P < 0.05$). Further, increased levels of branched-chain amino acids and amino acids of the glutamate and aspartate families were found in drought treatments (e.g. glutamine – needle lme: $pR^2 = 0.59$; root lme: $pR^2 = 0.77$; Tukey HSD, $P < 0.05$). A distinct response of the primary metabolome to $e[CO_2]$ under drought was remarkably absent in roots, whereas $e[CO_2]$ showed a tendency to mitigate metabolic responses to drought in needle tissues.

Heat stress responses affected by $[CO_2]$ and drought The temperature increase from $25^\circ C$ to $40^\circ C$ affected the primary metabolome in needles and roots differently (Fig. 7). A general trend in needle tissues was the decrease of carboxylic acids (lme: $pR^2 = 0.47$) and an increase of sugar alcohols (e.g. pinitol, lme: $pR^2 = 0.65$; and galactinol, lme: $pR^2 = 0.59$), whereas *myo*-inositol decreased (lme: $pR^2 = 0.25$; Tukey HSD, $P < 0.05$). Secondary metabolite precursors such as putrescine (lme: $pR^2 = 0.37$), tyrosine, and phenylalanine also increased with temperature (lme: $pR^2 = 0.6–0.84$) relatively uniformly among treatments. Responses to increasing temperatures became most obvious in the root tissues (Fig. 7), where we found amino acids (glutamine, asparagine, alanine, serine, threonine, valine, and isoleucine) to accumulate with rising temperatures (lme: $pR^2 = 0.6–0.8$). This increase was marked under $a[CO_2]$ in both drought and well-watered trees along with a decline in root

Fig. 7 Principal components analysis of all quantified 38 primary metabolites in shoot and root tissues (*Pinus halepensis*) at 25°C (closed symbols) and at 40°C (open symbols) per treatment. Polygons indicate treatment clustering. Inset: visualization of overall changes in root (brown symbols) and needle (green symbols) tissues irrespective of treatment and temperature. Note that all metabolite data were scaled to SD (see the Materials and Methods section). Metabolite abbreviations: Gluc, glucose; Fruc, fructose; Gal, galactose; Suc, sucrose; Treh, trehalose; Malt, maltose; Mel, melibiose; Raf, raffinose; Inos, *myo*-inositol; Pini, pinitol; Galact, galactinol; Threi, threitol; Oxoglu, 2-oxoglutarate; Oxaloac, oxaloacetate; Citr, citrate; Mal, malate; Succ, succinate; Fum, fumarate; Pyruv, pyruvate; Thrnate, threonate; Glu, glutamate; Gln, glutamine; Asp, aspartate; Asn, asparagine; Gly, glycine; Ala, alanine; Ser, serine; Ile, isoleucine; Leu, leucine; Val, valine; Thr, threonine; Pro, proline; Lys, lysine; Met, methionine; Tyr, tyrosine; Phe, phenylalanine; Trp, tryptophane; Putr, putrescine.



protein (lme: $pR^2 = 0.38$; Fig. 8t). By contrast, needle protein increased above 35°C in all treatments (Fig. 8t), particularly under e[CO₂]D (lme: $pR^2 = 0.23$; Tukey HSD, $P < 0.05$). In addition, treatment-specific responses to temperature were found in monosaccharides (lme: $pR^2 = 0.74$), where drought resulted in an accumulation of monosaccharides in needles (Tukey HSD, $P < 0.05$; Fig. 8a,b). In the well-watered treatments, we found monosaccharides to decline in roots (Fig. 8c,d; lme: $pR^2 = 0.70$; Tukey HSD, $P < 0.05$). This decline tended to be greater in trees grown under a[CO₂].

Discussion

Tree C balance under e[CO₂]

Aleppo pine trees grown for 1.5 yr under e[CO₂] exhibited a larger biomass than trees grown under a[CO₂]. We cannot exclude limiting effects on growth due to the size of the pots, which were lower than what has been previously recommended (Poorter *et al.*, 2012). Nevertheless, we found clear differences in root biomass and e[CO₂] to stimulate root growth, in agreement with many other studies (for a meta-analysis of free-air CO₂ enrichment studies, see Nie *et al.*, 2013). The observed overall larger biomass of e[CO₂] trees in our study tended to result in a larger net C gain (i.e. net photosynthesis minus respiration; on average, +120% per tree). To exclude the CO₂-induced biomass stimulation on these results, we expressed gas-exchange rates per tissue DW. Based thereon, we did not find e[CO₂] to increase C-fixation rates, as A_{Net} was quite similar between the two [CO₂] treatments (Table 2), and carboxylation efficiency was unchanged (data not shown). Hence, the stimulation of the seedlings' net C gain in the e[CO₂]W treatment was not driven by increased photosynthesis but due to an apparent reduction of R_{Shoot} and R_{Root}

under e[CO₂] (−23% on average). It is noteworthy that, under drought conditions, [CO₂] did not affect respiration rates.

The responses of respiration to e[CO₂] can be highly variable (Dusenge, 2019). Some studies find respiration to be insensitive to [CO₂], whereas others find it to either increase or decrease (Drake *et al.*, 1999; Gonzalez-Meler *et al.*, 2004; Ainsworth & Long, 2005; Gauthier *et al.*, 2014; Xu *et al.*, 2015; Aspinwall *et al.*, 2017; Dusenge *et al.*, 2019). Our study adds new evidence that e[CO₂] reduces R_{Shoot} or R_{Root} per tissue DW (day and nighttime) during nonstressful conditions. Correspondingly, we also did not find an upregulation of respiratory substrates such as sugars in response to e[CO₂]. A likely explanation for reduced dark respiration in response to rising [CO₂] may involve lower protein turnover due to N dilution from increases in nonstructural carbohydrates or other organic compounds (Xu *et al.*, 2015); yet, in our study, the C : N ratio at 25°C derived from the sum of primary metabolites did not differ (Table S2). However, we found evidence that e[CO₂] reduced protein content in needle and root tissues at the control temperature. Indeed, the CO₂ effect (at 25°C) disappeared when expressing R_{Shoot} per protein content. Because protein turnover is highly energy demanding, a lower protein content of plants under e[CO₂] could reduce the respiratory costs of tissue maintenance (Drake *et al.*, 1999) and may contribute to increased net C uptake under well-watered conditions.

Temperature acclimation of respiration affects tree C balance and is modulated by drought and [CO₂]

The response of respiration to slowly increasing temperatures and VPD did not follow temperature kinetics of a single enzyme, which is exponential in a physiological temperature range (Bond-Lamberty *et al.*, 2004; Michaletz, 2018). By contrast, we found

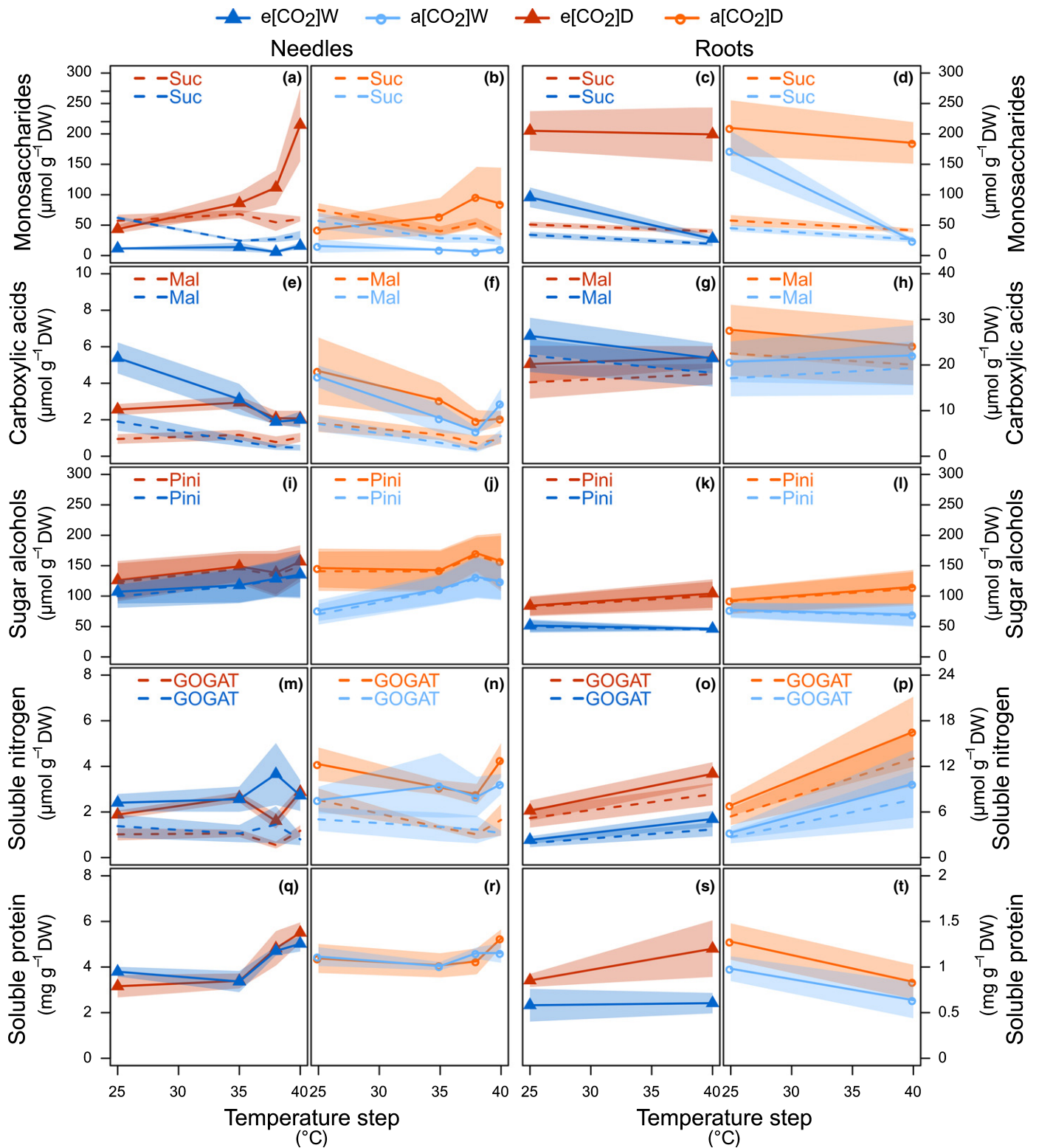


Fig. 8 Heat stress responses of selected primary metabolites and protein content in leaves and roots of *Pinus halepensis* seedlings. Shown are treatment averages of (a–d) sucrose and the sum of monosaccharides (glucose, fructose, and galactose), (e–h) malate and the sum of carboxylic acids (citrate, malate, fumarate, succinate, oxoglutarate, oxaloacetate), (i–l) pinitol and the sum of sugar alcohols (*myo*-inositol, pinitol, threitol, galactinol), (m–t) glutamate synthase amino acids (GOGAT) and the sum of (m–p) all measured amino acids including putrescine and (q–t) protein content. The shaded areas are ± 1 SE ($n = 8$).

respiration to acclimate to several days of heat stress. Moreover, we found that daytime respiration at 40°C was close to the initial rates at 25°C. This is in stark contrast to studies conducting fast temperature curves, which typically find respiratory peaks to occur at much higher temperatures (e.g. Gauthier *et al.*, 2014). However, an acclimation of leaf respiration to elevated growth temperatures has been reported in many instances (Reich *et al.*, 2016; Drake *et al.*, 2019), and R_{Shoot} has been shown to decline during consecutive heatwaves (Birami *et al.*, 2018). Likely explanations for the early downregulation of R_{Shoot} and R_{Root} that we have found in response to heat stress are: first, reduced respiratory demand due to downregulation of growth and maintenance respiration; second, adenylate restriction caused by ATP turnover decline; and/or third, reduced C availability (O'Leary *et al.*, 2019). Though our study cannot support respiration to be limited by reduced C availability as, for instance, carboxylic acids did not decrease in root tissues, we can clearly show that Aleppo pine trees are able to regulate respiratory losses to maintain a new equilibrium between C loss and uptake (Fig. 4). This was reflected in the whole-tree C balance stabilizing at an almost constant rate between 35°C and 40°C, with larger net C loss under drought conditions. An homeostatic linkage between photosynthesis and respiration to temperature has been suggested by a recent synthesis on a large number of studies (Dusenge *et al.*, 2019).

The impacts of $e[\text{CO}_2]$ on respiration vanished with increasing heat stress in the well-watered trees; and after the respiratory peaks were reached, on average 1–2°C later under $e[\text{CO}_2]$, respiration did not differ between the $[\text{CO}_2]$ treatments anymore. However, the effect of drought delaying the timing of the respiratory peak was more pronounced. Respiration was initially lower under drought until maximum rates were reached *c.* 2–6°C later than in the well-watered trees. The subsequent decline in respiration under drought was less pronounced, so that respiration of the drought and well-watered treatments converged. A similar delay of the respiratory peak in response to drought (although at much higher temperatures) has been found during rapid warming of eucalypt leaves (Gauthier *et al.*, 2014). In accordance with Gauthier *et al.* (2014), we found a declining ratio of A_{Net} to respiration but no indications for C depletion. In summary, this indicated that treatment differences (e.g. drought or $[\text{CO}_2]$) in respiration were distinct at 25°C, but quickly subsided after maximum temperatures were surpassed. The underlying reasons are not clear; but strikingly, the trees maintained a new equilibrium between A_{Net} and respiration, and whole-tree net C loss in the well-watered treatments was $< 0.1\% \text{ DW d}^{-1}$ and in the drought treatments $< 0.2\% \text{ DW d}^{-1}$, independent of the $[\text{CO}_2]$.

Responses of WUE to elevated $[\text{CO}_2]$, heat, and drought stress

The apparent lack of a $[\text{CO}_2]$ effect on net C uptake under stress was counterbalanced by a very consistent H_2O -saving strategy, largely maintained throughout all temperature steps (Table S3). In the well-watered $e[\text{CO}_2]$ trees, E remained constant with

increasing VPD and temperature. This was reflected in an improved WUE under $e[\text{CO}_2]$, which increased proportionally with $a[\text{CO}_2]$ under well-watered conditions. Moreover, this increase in WUE was not only maintained but apparently increased with rising temperatures (on average, +77% at 25°C, 94% at 30°C, 95% at 35°C, and 133% at 40°C) and, therefore, agrees with our second hypothesis. Several strategies are reported to control WUE in plants (Lavergne *et al.*, 2019); and under rising C_a , three scenarios are typically proposed in which leaves maintain either constant C_i , constant $C_a - C_i$, or constant $C_i : C_a$ (Saurer *et al.*, 2004). A variety of studies have reported constant $C_i : C_a$ as a response to $e[\text{CO}_2]$ during drought or other abiotic stresses (Ainsworth & Long, 2005; Kauwe *et al.*, 2013; Gimeno *et al.*, 2016). This agrees with our study, where $C_i : C_a$ remained almost constant over the entire experimental temperature gradient in the well-watered seedlings. Constant $C_i : C_a$ could indicate a feedback control on g_s from photosynthetic activity, for instance via temperature-induced downregulation of Rubisco (Crafts-Brandner & Salvucci, 2000). We observed similar $C_i : C_a$ patterns in the drought treatments, with a tendency for a larger increase in WUE at 25°C. This H_2O -saving effect naturally disappeared when stomata closed almost fully at 30°C. Thus, hot drought quickly diminishes any H_2O -saving effect of $e[\text{CO}_2]$.

Plant stress responses affected by elevated $[\text{CO}_2]$

Whole-tree gas-exchange of H_2O and CO_2 revealed some interacting $[\text{CO}_2]$ responses during drought and heat stress, most pronouncedly reflected in increased WUE. However, we found the benefits of $e[\text{CO}_2]$ to vanish under more extreme heat or combined heat–drought stress. Recently, it has been shown that extreme drought can counterbalance any beneficial $[\text{CO}_2]$ effects on C dynamics and H_2O relations (Duan *et al.*, 2013, 2015). In addition, more detrimental effects and larger leaf senescence in trees grown under $e[\text{CO}_2]$ compared with $a[\text{CO}_2]$ have been found during a hot drought event occurring naturally (Warren *et al.*, 2011). The underlying mechanisms are not yet understood, but excessive leaf-temperature stress under $e[\text{CO}_2]$ due to lower g_s (and lower E) are thought to be a possible explanation, increasing thermal stress (Bassow *et al.*, 1994; Warren *et al.*, 2011). As the well-mixed conditions inside the tree chambers in our study omitted large differences in surface needle temperatures (Table S1), we can exclude additional heating of $e[\text{CO}_2]$ trees affecting metabolic stress responses.

Underlying mechanisms for the rather modest effect of $[\text{CO}_2]$ on tree stress performance might be reflected in metabolic adjustments in needles and roots. Generally, we found the primary metabolome of roots and shoots to differ, which can be explained by the presence or absence of chemical pathways in specialized tissues like plastids (Li *et al.*, 2016). Elevated $[\text{CO}_2]$ tended to mitigate the drought response at 25°C in needle tissues, which fits well to overall H_2O -saving strategy (e.g. WUE; see Table 2). However, the response to heat stress was distinct but not altered by $e[\text{CO}_2]$. For instance, we found *myo*-inositol to decline as a typical precursor of osmotic active substances like pinitol and galactinol (Nishizawa *et al.*, 2008). Together with proline, these

metabolites contribute to thermostability of membranes and proteins (Nishizawa *et al.*, 2008; Zinta *et al.*, 2018). In contrast to needles, root metabolites showed distinct responses to stress, as seen in highly elevated levels of soluble sugars and amino acid increase with heat and drought stress. The apparently greater drought sensitivity of roots was also reflected by a lower root biomass but higher overall metabolite C content than in the well-watered trees (Table 1), indicating that root growth halted during drought and that available C was mainly invested into osmoregulation. Possible explanations may involve reduced C transport from source to sink tissues (Ruehr *et al.*, 2016; Brauner *et al.*, 2018) and a larger hydraulic vulnerability of roots (Johnson *et al.*, 2016).

We found some indications for e[CO₂] to potentially mitigate stress-induced metabolic responses, in agreement with others (Zinta *et al.*, 2014, 2018). In particular, e[CO₂] seemed to lessen the heat-induced changes in monosaccharides and amino acids in roots. Similarly, Zinta *et al.* (2018) reported a dampened response of sugars and amino acids to combined heat–drought stress in *Arabidopsis thaliana* grown under e[CO₂]. Hence, the larger increase in amino acid concentrations in roots from trees grown under a[CO₂] in our study could be triggered by protein degradation, which was suggested by a decline in protein content while asparagine accumulated (Brouquisse *et al.*, 1992). Heat stress has been found to decrease root protein content, as protein degradation rates at high temperatures typically exceed protein synthesis (Huang *et al.*, 2012). A greater protein stability is assumed to improve the thermotolerance of plants but may come at the cost of increased maintenance. Interestingly, we found a greater stability of root protein content under e[CO₂] with heat stress, but the average root protein content as well as R_{root} at 40°C did not differ between a[CO₂]W and e[CO₂]W. This may indicate an active downregulation of protein turnover in a[CO₂] trees to reduce the C cost of maintenance respiration. Counterintuitively, we found protein content in needle tissues to increase at temperatures $\geq 35^\circ\text{C}$ in all treatments. It is noteworthy that e[CO₂] trees, which had a lower protein content at 25°C, exhibited a relatively greater increase in protein content with heat stress. This increase in soluble protein might be due to an upregulation of heat-shock proteins (Aspinwall *et al.*, 2019) to prevent failure of the photosynthetic apparatus (Escandón *et al.*, 2017) or could be caused by N remobilization for Rubisco, which can explain up to 30% of changes in total protein (Warren & Adams, 2001). In summary, we found the stress response of the primary metabolome to be highly tissue specific and to be largely independent of growth [CO₂] in contrast to our third hypothesis. However, we detected some indications for a slightly enhanced thermotolerance under e[CO₂] reflected in a larger upregulation of needle proteins and improved stability of root proteins, at the expense of lower amino acid accumulation.

Conclusion

Growing Aleppo pines for 18 months under e[CO₂] of *c.* 870 ppm had a stimulating effect on tree biomass (+40%), but did not result in larger tree H₂O loss due to reductions in

stomatal conductance reflected in a nearly proportional increase in WUE maintained throughout a 10 d heatwave (25°C, 30°C, 35°C, 38°C, 40°C). Drought stress initially amplified the e[CO₂] effect on WUE until stomata closed at higher temperatures. Considering the tree C balance, we found a stimulation of the net C uptake under e[CO₂] largely due to reduced tissue respiration alongside lower protein content. Nevertheless, respiration responded independent of [CO₂] to heat stress with an initial increase followed by a decline above 31–34°C. Photosynthesis decreased simultaneously, and the trees started to lose C above 30°C, irrespective of [CO₂]. Elevated [CO₂] had only a modest effect on the stress response of the primary metabolome, which differed among tissues. Interactive effects between [CO₂] and heat stress became visible via lower protein degradation in roots under e[CO₂], indicating an improved thermotolerance. In summary, we could show that a doubling of atmospheric [CO₂] has little influence on Aleppo pine seedling responses to heat, drought, or hot drought stress. Though our study is restricted to physiological responses of seedlings, the results have implications for model development, which are two-fold: the effect of atmospheric [CO₂] on tree physiological responses decreases with stress intensity, such as hot drought; and respiration acclimates to heat stress within days and the relationship with temperature is independent of [CO₂] but altered by drought. In order to more accurately assess mitigating effects of e[CO₂] on drought stress responses of Mediterranean-type forests, e[CO₂]-induced changes of whole tree C allocation affecting tree H₂O uptake and H₂O loss need to be considered.

Acknowledgements

We would like to thank Andrea-Livia Jakab, Lisa Fürtauer, and Romy Rehschuh for assistance with the experimental set-up and lab work and Daniel Nadal-Sala for help with statistical analyses. We are also grateful to Dan Yakir and his team members for access to the Yatir research site and fruitful scientific discussions. Further, we would like to thank Wolfram Weckwerth and the Department of Molecular Systems Biology (University of Vienna, Austria) who provided us with the expertise and the infrastructure to conduct the metabolome analysis. This work was supported by the German Research Foundation through its German–Israeli project cooperation program (SCHM 2736/2-1 and YA 274/1-1) and by the German Federal Ministry of Education and Research, through the Helmholtz Association and its research program ATMO. BB received additional support from the Graduate School for Climate and Environment, and NKR acknowledges support from the German Research Foundation through its Emmy Noether Program (RU 1657/2-1).

Author contributions

AA, BB and NKR designed the study. BB conducted the experiment and analyzed the data with support from AG, MG, TN, YP and NKR. BB and NKR wrote the paper with contributions from all co-authors.

Data availability statement

The gas-exchange data have been made available through PANGAEA® Data Publisher for Earth & Environmental Science: <https://doi.pangaea.de/10.1594/PANGAEA.910582>. Metabolite data will be made available upon request.

ORCID

Almut Arneith  <https://orcid.org/0000-0001-6616-0822>
Benjamin Birami  <https://orcid.org/0000-0002-0142-8418>
Marielle Gattmann  <https://orcid.org/0000-0001-5035-928X>
Thomas Nägele  <https://orcid.org/0000-0002-5896-238X>
Yakir Preisler  <https://orcid.org/0000-0001-5861-8362>
Nadine K. Ruehr  <https://orcid.org/0000-0001-5989-7463>

References

- Ainsworth EA, Long SP. 2005. What have we learned from 15 years of free-air CO₂ enrichment (FACE)? A meta-analytic review of the responses of photosynthesis, canopy properties and plant production to rising CO₂. *New Phytologist* 165: 351–371.
- Ainsworth EA, Rogers A. 2007. The response of photosynthesis and stomatal conductance to rising CO₂: mechanisms and environmental interactions. *Plant, Cell & Environment* 30: 258–270.
- Akaike H. 1974. A new look at the statistical model identification. *IEEE Transactions on Automatic Control* 19: 716–723.
- Amey M, Wertin TM, Bauweraerts I, McGuire MA, Teskey RO, Steppe K. 2012. The effect of induced heat waves on *Pinus taeda* and *Quercus rubra* seedlings in ambient and elevated CO₂ atmospheres. *New Phytologist* 196: 448–461.
- Anderegg WRL, Kane JM, Anderegg LDL. 2013. Consequences of widespread tree mortality triggered by drought and temperature stress. *Nature Climate Change* 3: 30–36.
- Aspinwall MJ, Jacob VK, Blackman CJ, Smith RA, Tjoelker MG, Tissue DT. 2017. The temperature response of leaf dark respiration in 15 provenances of *Eucalyptus grandis* grown in ambient and elevated CO₂. *Functional Plant Biology* 44: 1075–1086.
- Aspinwall MJ, Pfautsch S, Tjoelker MG, Vårhammar A, Possell M, Drake JE, Reich PB, Tissue DT, Atkin OK, Rymer PD *et al.* 2019. Range size and growth temperature influence *Eucalyptus* species responses to an experimental heatwave. *Global Change Biology* 25: 1665–1684.
- Atkin O, Tjoelker MG. 2003. Thermal acclimation and the dynamic response of plant respiration to temperature. *Trends in Plant Science* 8: 343–351.
- Baldwin JW, Dessy JB, Vecchi GA, Oppenheimer M. 2019. Temporally compound heat wave events and global warming: an emerging hazard. *Earth's Future* 7: 411–427.
- Barton K. 2019. *MuMIn: multi-model inference*. R package v.1.43.10. [WWW document] URL <https://CRAN.R-project.org/package=MumIn> [accessed 5 December 2019].
- Bassow SL, McConnaughay KDM, Bazzaz FA. 1994. The response of temperate tree seedlings grown in elevated CO₂ to extreme temperature events. *Ecological Applications* 4: 593–603.
- Birami B, Gattmann M, Heyer AG, Grote R, Arneith A, Ruehr NK. 2018. Heat waves alter carbon allocation and increase mortality of Aleppo pine under dry conditions. *Frontiers in Forests and Global Change* 1: e1285.
- Bond-Lamberty B, Wang C, Gower ST. 2004. Contribution of root respiration to soil surface CO₂ flux in a boreal black spruce chronosequence. *Tree Physiology* 24: 1387–1395.
- Brauner K, Birami B, Brauner HA, Heyer AG. 2018. Diurnal periodicity of assimilate transport shapes resource allocation and whole-plant carbon balance. *The Plant Journal* 94: 776–789.
- Brouquisse R, James F, Pradet A, Raymond P. 1992. Asparagine metabolism and nitrogen distribution during protein degradation in sugar-starved maize root tips. *Planta* 188: 384–395.
- Choat B, Brodrribb TJ, Brodersen CR, Duursma RA, López R, Medlyn BE. 2018. Triggers of tree mortality under drought. *Nature* 558: 531–539.
- Coleman JS, Rochefort L, Bazzaz FA, Woodward FI. 1991. Atmospheric CO₂, plant nitrogen status and the susceptibility of plants to an acute increase in temperature. *Plant, Cell & Environment* 14: 667–674.
- Coumou D, Rahmstorf S. 2012. A decade of weather extremes. *Nature Climate Change* 2: 491–496.
- Crafts-Brandner SJ, Salvucci ME. 2000. Rubisco activase constrains the photosynthetic potential of leaves at high temperature and CO₂. *Proceedings of the National Academy of Sciences, USA* 97: 13430–13435.
- de Kauwe MG, Medlyn BE, Zaehle S, Walker AP, Dietze MC, Hickler T, Jain AK, Luo Y, Parton WJ, Prentice IC *et al.* 2013. Forest water use and water use efficiency at elevated CO₂. A model-data intercomparison at two contrasting temperate forest FACE sites. *Global Change Biology* 19: 1759–1779.
- de Simón BF, Cahalía E, Aranda I. 2018. Metabolic response to elevated CO₂ levels in *Pinus pinaster* Aiton needles in an ontogenetic and genotypic-dependent way. *Plant Physiology and Biochemistry* 132: 202–212.
- Drake BG, Azcon-Bieto J, Berry J, Bunce J, Dijkstra P, Farrar J, Gifford RM, Gonzalez-Meler MA, Koch G, Lambers H *et al.* 1999. Does elevated atmospheric CO₂ concentration inhibit mitochondrial respiration in green plants? *Plant, Cell & Environment* 22: 649–657.
- Drake JE, Furze ME, Tjoelker MG, Carrillo Y, Barton CVM, Pendall E. 2019. Climate warming and tree carbon use efficiency in a whole-tree ¹³C₂ tracer study. *New Phytologist* 222: 1313–1324.
- Duan H, Amthor JS, Duursma RA, O'Grady AP, Choat B, Tissue DT. 2013. Carbon dynamics of eucalypt seedlings exposed to progressive drought in elevated CO₂ and elevated temperature. *Tree Physiology* 33: 779–792.
- Duan H, Duursma RA, Huang G, Smith RA, Choat B, O'Grady AP, Tissue DT. 2014. Elevated CO₂ does not ameliorate the negative effects of elevated temperature on drought-induced mortality in *Eucalyptus radiata* seedlings. *Plant, Cell & Environment* 37: 1598–1613.
- Duan H, O'Grady AP, Duursma RA, Choat B, Huang G, Smith RA, Jiang Y, Tissue DT. 2015. Drought responses of two gymnosperm species with contrasting stomatal regulation strategies under elevated [CO₂] and temperature. *Tree Physiology* 35: 756–770.
- Dusenge ME, Duarte AG, Way DA. 2019. Plant carbon metabolism and climate change: elevated CO₂ and temperature impacts on photosynthesis, photorespiration and respiration. *New Phytologist* 221: 32–49.
- Eamus D. 1991. The interaction of rising CO₂ and temperatures with water use efficiency. *Plant, Cell & Environment* 14: 843–852.
- Escandón M, Valledor L, Pascual J, Pinto G, Cañal MJ, Meijón M. 2017. System-wide analysis of short-term response to high temperature in *Pinus radiata*. *Journal of Experimental Botany* 68: 3629–3641.
- Fürtauer L, Küstner L, Weckwerth W, Heyer AG, Nägele T. 2019. Resolving subcellular plant metabolism. *The Plant Journal* 100: 438–455.
- Fürtauer L, Pschenitschnigg A, Scharhosi H, Weckwerth W, Nägele T. 2018. Combined multivariate analysis and machine learning reveals a predictive module of metabolic stress response in *Arabidopsis thaliana*. *Molecular Omics* 14: 437–449.
- Fürtauer L, Weckwerth W, Nägele T. 2016. A benchtop fractionation procedure for subcellular analysis of the plant metabolome. *Frontiers in Plant Science* 7: e1912.
- Gauthier PPG, Crous KY, Ayub G, Duan H, Weerasinghe LK, Ellsworth DS, Tjoelker MG, Evans JR, Tissue DT, Atkin OK. 2014. Drought increases heat tolerance of leaf respiration in *Eucalyptus globulus* saplings grown under both ambient and elevated atmospheric CO₂ and temperature. *Journal of Experimental Botany* 65: 6471–6485.
- Gimeno TE, Crous KY, Cooke J, O'Grady AP, Ósváldsson A, Medlyn BE, Ellsworth DS. 2016. Conserved stomatal behaviour under elevated CO₂ and varying water availability in a mature woodland. *Functional Ecology* 30: 700–709.
- Giraud C. 2015. *Introduction to high-dimensional statistics*. Boca Raton, FL, USA: CRC Press.

- Gonzalez-Meler MA, Taneva L, Trueman RJ. 2004. Plant respiration and elevated atmospheric CO₂ concentration: cellular responses and global significance. *Annals of Botany* 94: 647–656.
- Grünzweig JM, Hemming D, Maseyk K, Lin T, Rotenberg E, Raz-Yaseef N, Falloon PD, Yakir D. 2009. Water limitation to soil CO₂ efflux in a pine forest at the semiarid “timberline”. *Journal of Geophysical Research* 114: 10823.
- Hamerlynck EP, Huxman TE, Loik ME, Smith SD. 2000. Effects of extreme high temperature, drought and elevated CO₂ on photosynthesis of the Mojave Desert evergreen shrub, *Larrea tridentata*. *Plant Ecology* 148: 183–193.
- Hartmann H, Trumbore S. 2016. Understanding the roles of nonstructural carbohydrates in forest trees – from what we can measure to what we want to know. *New Phytologist* 211: 386–403.
- Hsiao TC. 1973. Plant responses to water stress. *Annual Reviews of Plant Physiology* 24: 519–570.
- Huang B, Rachmilevitch S, Xu J. 2012. Root carbon and protein metabolism associated with heat tolerance. *Journal of Experimental Botany* 63: 3455–3465.
- IPCC. 2014. Pachauri RK, Meyer LA, Barros VR, Broome J, Cramer W, Crist R, Church JR, Clarke L, Dahe Dahe Q, Dasgupta P (eds). *Climate change 2014: synthesis report. Contribution of Working Groups I, II and III to the Fifth Assessment Report of the Intergovernmental Panel on Climate Change*. Geneva, Switzerland: IPCC.
- Johnson DM, Wortemann R, McCulloh KA, Jordan-Meille L, Ward E, Warren JM, Palmroth S, Domec JC. 2016. A test of the hydraulic vulnerability segmentation hypothesis in angiosperm and conifer tree species. *Tree Physiology* 36: 983–993.
- Johnson RM, Pregitzer KS. 2007. Concentration of sugars, phenolic acids, and amino acids in forest soils exposed to elevated atmospheric CO₂ and O₃. *Soil Biology and Biochemistry* 39: 3159–3166.
- Kuznetsova A, Brockhoff PB, Christensen RHB. 2017. *LMERTEST* package. *Tests in linear mixed effects models*. R package v.3.1.0. [WWW document] URL <https://CRAN.R-project.org/package=lmerTest> [accessed 21 January 2019].
- Lavergne A, Graven H, de Kauwe MG, Keenan TF, Medlyn BE, Prentice IC. 2019. Observed and modelled historical trends in the water-use efficiency of plants and ecosystems. *Global Change Biology* 25: 2242–2257.
- Li D, Heiling S, Baldwin IT, Gaquerel E. 2016. Illuminating a plant’s tissue-specific metabolic diversity using computational metabolomics and information theory. *Proceedings of the National Academy of Sciences, USA* 113: 7610–7618.
- Maechler M, Rousseeuw P, Struyf A, Hubert M, Hornik K. 2018. *CLUSTER: cluster analysis basic and extensions*. R package v.2.0.7-1. [WWW document] URL <https://CRAN.R-project.org/package=cluster> [accessed 20 December 2018].
- Michaletz ST. 2018. Evaluating the kinetic basis of plant growth from organs to ecosystems. *New Phytologist* 219: 37–44.
- Mohanta TK, Bashir T, Hashem A, Abd A, Elsayed F. 2017. Systems biology approach in plant abiotic stresses. *Plant Physiology and Biochemistry* 121: 58–73.
- Nie M, Lu M, Bell J, Raut S, Pendall E. 2013. Root traits at elevated CO₂. *Global Ecology and Biogeography* 22: 1095–1105.
- Nishizawa A, Yabuta Y, Shigeoka S. 2008. Galactinol and raffinose constitute a novel function to protect plants from oxidative damage. *Plant Physiology* 147: 1251–1263.
- O’Leary BM, Asao S, Millar AH, Atkin OK. 2019. Core principles which explain variation in respiration across biological scales. *New Phytologist* 222: 670–686.
- Pfleiderer P, Schleussner C, Kornhuber K, Coumou D. 2019. Summer weather becomes more persistent in a 2°C world. *Nature Climate Change* 9: 666–671.
- Poorter H, Bühler J, van Dusschoten D, Climent J, Postma JA. 2012. Pot size matters: a meta-analysis of the effects of rooting volume on plant growth. *Functional Plant Biology* 39: 839–850.
- Poorter H, van Berkel Y, Baxter R, Den Hertog J, Dijkstra P, Gifford RM, Griffin KL, Roumet C, Roy J, Wong SC. 1997. The effect of elevated CO₂ on the chemical composition and construction costs of leaves of 27 C₃ species. *Plant, Cell & Environment* 20: 472–482.
- R Core Team. 2018. *R. A language and environment for statistical computing*. Version 3.5.2 (201812-20). R Foundation for Statistical Computing, Vienna, Austria. [WWW document] URL <https://www.R-project.org/>.
- Reich PB, Sendall KM, Stefanski A, Wei X, Rich RL, Montgomery RA. 2016. Boreal and temperate trees show strong acclimation of respiration to warming. *Nature* 531: 633–636.
- Ruehr NK, Gast A, Weber C, Daub B, Arneth A. 2016. Water availability as dominant control of heat stress responses in two contrasting tree species. *Tree Physiology* 36: 164–178.
- Ryan MG, Asao S. 2019. Clues for our missing respiration model. *New Phytologist* 222: 1167–1170.
- Saurer M, Siegwolf RTW, Schweingruber FH. 2004. Carbon isotope discrimination indicates improving water-use efficiency of trees in northern Eurasia over the last 100 years. *Global Change Biology* 10: 2109–2120.
- Simón BF, de Cadahía E, Aranda I. 2018. Metabolic response to elevated CO₂ levels in *Pinus pinaster* Aiton needles in an ontogenetic and genotypic-dependent way. *Plant Physiology and Biochemistry* 132: 202–212.
- Spieß AN. 2018. *PROPAGATE: propagation of uncertainty*. R package v.1.0-6. [WWW document] URL <https://CRAN.R-project.org/package=propagate> [accessed 21 January 2019].
- Tatarinov F, Rotenberg E, Maseyk K, Ogée J, Klein T, Yakir D. 2016. Resilience to seasonal heat wave episodes in a Mediterranean pine forest. *New Phytologist* 210: 485–496.
- Tyree MT, Zimmermann MH. 2002. Hydraulic architecture of whole plants and plant performance. In: Timell TE, Tyree MT, Zimmermann MH, eds. *Xylem structure and the ascent of sap*. Berlin, Germany: Springer, 175–214.
- Warren CR, Adams MA. 2001. Distribution of N, Rubisco and photosynthesis in *Pinus pinaster* and acclimation to light. *Plant, Cell & Environment* 24: 597–609.
- Warren JM, Norby RJ, Wullschlegel SD. 2011. Elevated CO₂ enhances leaf senescence during extreme drought in a temperate forest. *Tree Physiology* 31: 117–130.
- Weiszmann J, Fürtauer L, Weckwerth W, Nägele T. 2018. Vacuolar sucrose cleavage prevents limitation of cytosolic carbohydrate metabolism and stabilizes photosynthesis under abiotic stress. *FEBS Journal* 285: 4082–4098.
- Wickham H. 2016. *GGPLOT2: elegant graphics for data analysis*. R package v.3.1.0 [WWW document] URL <http://ggplot2.org> [accessed 21 January 2019].
- Williams AP, Allen CD, Macalady AK, Griffin D, Woodhouse CA, Meko DM, Swetnam TW, Rauscher SA, Seager R, Grissino-Mayer HD *et al.* 2013. Temperature as a potent driver of regional forest drought stress and tree mortality. *Nature Climate Change* 3: 292–297.
- Wullschlegel SD, Tschaplinski TJ, Norby RJ. 2002. Plant water relations at elevated CO₂ – implications for water-limited environments. *Plant, Cell & Environment* 25: 319–331.
- Xu Z, Jiang Y, Zhou G. 2015. Response and adaptation of photosynthesis, respiration, and antioxidant systems to elevated CO₂ with environmental stress in plants. *Frontiers in Plant Science* 6: e701.
- Zhang X, Högy P, Wu X, Schmid I, Wang X, Schulze WX, Jian D, Fangmeier A. 2018. Physiological and proteomic evidence for the interactive effects of post-anthesis heat stress and elevated CO₂ on wheat. *Proteomics* 18: e1800262.
- Zhao J, Hartmann H, Trumbore S, Ziegler W, Zhang Y. 2013. High temperature causes negative whole-plant carbon balance under mild drought. *New Phytologist* 200: 330–339.
- Zinta G, AbdElgawad H, Domagalska MA, Vergauwen L, Knapen D, Nijs I, Janssens IA, Beeemster GTS, Asard H. 2014. Physiological, biochemical, and genome-wide transcriptional analysis reveals that elevated CO₂ mitigates the impact of combined heat wave and drought stress in *Arabidopsis thaliana* at multiple organizational levels. *Global Change Biology* 20: 3670–3685.
- Zinta G, AbdElgawad H, Peshev D, Weedon JT, van den Ende W, Nijs I, Janssens IA, Beeemster GTS, Asard H. 2018. Dynamics of metabolic responses to periods of combined heat and drought in *Arabidopsis thaliana* under ambient and elevated atmospheric CO₂. *Journal of Experimental Botany* 69: 2159–2170.

Supporting Information

Additional Supporting Information may be found online in the Supporting Information section at the end of the article.

Fig. S1 Growth conditions of Aleppo pine seedlings.

Fig. S2 Soil moisture conditions during seedling cultivation.

Fig. S3 Temperature responses of midday needle water potential (ψ_{needle}).

Fig. S4 Temperature responses of water use efficiency and stomatal conductance.

Fig. S5 Clustered dendrogram analysis of metabolite responses (25°C).

Notes S1 Tree gas exchange chamber system.

Notes S2 Primary metabolite and protein analyses.

Table S1 Needle surface temperatures.

Table S2 Soluble carbon (C) and soluble nitrogen (N) content.

Table S3 Treatment averages of daily tree transpiration given per temperature step.

Please note: Wiley Blackwell are not responsible for the content or functionality of any Supporting Information supplied by the authors. Any queries (other than missing material) should be directed to the *New Phytologist* Central Office.



About *New Phytologist*

- *New Phytologist* is an electronic (online-only) journal owned by the New Phytologist Trust, a **not-for-profit organization** dedicated to the promotion of plant science, facilitating projects from symposia to free access for our Tansley reviews and Tansley insights.
- Regular papers, Letters, Research reviews, Rapid reports and both Modelling/Theory and Methods papers are encouraged. We are committed to rapid processing, from online submission through to publication 'as ready' via *Early View* – our average time to decision is <26 days. There are **no page or colour charges** and a PDF version will be provided for each article.
- The journal is available online at Wiley Online Library. Visit **www.newphytologist.com** to search the articles and register for table of contents email alerts.
- If you have any questions, do get in touch with Central Office (np-centraloffice@lancaster.ac.uk) or, if it is more convenient, our USA Office (np-usaoffice@lancaster.ac.uk)
- For submission instructions, subscription and all the latest information visit **www.newphytologist.com**